THE ASTROPHYSICAL JOURNAL, 200:269–277, 1975 September 1

ORBITAL ELEMENTS AND AN ANALYSIS OF MODELS FOR HDE 226868 = CYGNUS X-1

C. T. BOLTON
David Dunlap Observatory, University of Toronto
Received 1974 August 5; revised 1975 March 5

ABSTRACT

Radial velocities from 21 new high-dispersion spectrograms of HDE 226868 are presented. These are combined with previously published data to calculate a "definitive" set of orbital elements for the binary system. In particular, archival data are used to obtain a precise period. The ellipsoidal light curve is analyzed using both a Roche model and an ellipsoidal model, and the results are compared with work by Hutchings. Information from the absorption-line and emission-line velocity curves and the light curve is combined to give estimates for the orbital inclination and the component masses. The possible errors in the analysis are discussed and are shown to be negligible. A qualitative model for the mass transfer is proposed that explains the intensity and velocity variations of the optical emission lines and the variations in the X-ray intensity—including the low-energy X-ray absorption events sometimes seen near superior conjunction of the secondary. Tests of this model are also proposed. Finally, the observations are used to test various models that have been proposed for the system. The observations rule out low mass and rotating degenerate dwarf secondaries and present difficulties for the triple star model. The magnetic reconnection model is not ruled out by the observations. Models in which the secondary is a black hole are consistent with all available observations.

Subject headings: binaries — stars, individual — X-ray sources

I. INTRODUCTION

The X-ray source Cygnus X-1 has been identified with the binary system HDE 226868 by Bolton (1971, 1972*a*) and Webster and Murdin (1972). These, and numerous other investigators (e.g., Cherepashchuk, Lyutyj, and Sunyaev 1972; Hutchings 1974*a*), have suggested that the X-rays from this system are produced by mass accretion onto a black hole secondary.[1] The recent detection of X-ray flux variability on time scales of approximately 1 ms (Rothschild *et al.* 1974) lends some support to these models.

At least four other models have been suggested for Cygnus X-1. These models attempt to account for the X-ray production in some way other than mass accretion onto a black hole. One class of these models removes the need for a black hole by reducing the mass of the system substantially below that implied by the spectral type of the primary, O9.7 Iab (Walborn 1973), and the normal mass-luminosity relation for supergiants (Stothers 1972). This can occur if the evolution of the stars has been affected by mass transfer in the binary system (e.g., Kippenhahn 1969). Another class of models accepts a large mass for the binary system but uses mechanisms other than mass accretion onto a black hole to produce the observed X-rays. In some of these models the secondary star is a normal main-sequence B star.

Most of these non-black hole models have been presented since the last comprehensive discussion of the optical observations of HDE 226868 (Bolton 1972*b*). A great many new optical and X-ray data have also become available during this period. Data from 23 new high-dispersion spectrograms are reported below, and these are used along with previously published data to derive "definitive" spectroscopic orbital elements. These elements, along with an independent analysis of the ellipsoidal light curve, are used to place limits on the dimensions of the binary system. A qualitative model is proposed for the mass transfer in the system, and the various models for the system are discussed.

[1] Throughout this paper the primary star will be identified with the visible star and the secondary star with the invisible companion.

II. ORBITAL ELEMENTS

a) New Data

Twenty-one new radial velocities for HDE 226868 are given in Table 1. These were measured from 12 Å mm^{-1} spectrograms taken with the 74-inch (1.9 m) telescope and Cassegrain grating spectrograph of the David Dunlap Observatory (DDO). Velocities are given for the absorption lines, He II λ4686 emission, Hβ emission, and the interstellar Ca II H and K lines separately. A qualitative estimate of the strength of the hydrogen emission is also given on these dates.

b) Spectroscopic Orbital Elements

The absorption-line velocities in Table 1 and those from Bolton (1972*b*), Webster and Murdin (1972), Hutchings *et al.* (1973), Brucato and Kristian (1973), and Smith, Margon, and Conti (1973) were used to derive the orbital elements. Some unpublished velocities from the Royal Greenwich Observatory (Mason

TABLE 1

NEW DDO RADIAL VELOCITIES

HELIOCENTRIC DATE (JD 2,440,000+)	ABS.	VELOCITY (km s^{-1}) p.e.	λ4686	Hβ	INTENSITY*	IS(Ca II)	NOTES
1534.693	+70.8	±1.4	−62	...	weak	−13.9	
						+98.8?	
1535.700	+32.0	1.4	...	...	—	−11.2	1
1558.632	−26.3	2.8	...	...	—	−12.9	
1765.867	−38.5	2.4	...	...	—	−14.5	
1797.817	+64.5	2.1	−97	...	—	−14.0	
1870.800	+79.2	2.2	−30	...	—	−11.0	
1871.722	− 2.4	2.6	...	−119	moderate	−11.8	2
1875.711	+73.9	1.6	−43	...	—	−14.4	
1886.783	+63.1	1.9	−38	...	—	−15.7	1
1887.702	+65.8	1.4	−70	...	—	−13.3	
1898.785	+76.2	2.8	−75	...	—	−11.2	
						+136.1	
1899.669	+16.4	1.8	...	...	—	−14.3	
1905.675	−13.9	2.2	...	...	moderate	− 7.1	
1907.637	−61.6	1.8	+75	...	—	−12.8	
1923.591	−71.8	3.0	+132	...	—	−10.4	
1928.588	−55.4	1.6	...	...	—	−14.1	
1930.580	−13.3	1.9	...	...	—	−19.4	
1930.695	− 9.0	2.3	...	...	—	−17.6	
1947.547	+ 3.6	3.8	...	...	—	−16.5	
1956.621	−40.9	1.2	...	...	—	−17.8	
2155.840	+73.1	2.6	−36	...	—	−18.5	

* A dash indicates no emission was noted.

NOTES.—(1) poor focus; (2) underexposed.

et al. 1974) were also used. Solutions were also tried with velocities from the He I λ6678 (Brucato and Zappala 1974) and He I λ5875 lines (Cowley 1974) included. These solutions failed to converge satisfactorily—apparently because the red helium-line velocities deviate markedly from Keplerian motion at certain phases. This deviation is largest just before the velocity extrema are reached and is in the sense that the red velocities give a larger velocity amplitude than the blue velocities.

The orbital elements were computed using a modified version of the program developed by Bertiau and Grobben (1969). In order to allow for systematic errors in the observations, the center-of-mass velocity V_0 was determined as a separate element for each set of velocities obtained with a different spectrograph. The velocities from the Mount Wilson and Palomar and Lick Observatories were taken with a variety of spectrographs, and not enough data exist to define V_0 separately for each spectrograph, so these velocities were combined to determine a single V_0. All velocities were weighted according to the scheme used previously by Bolton (1972*b*). Several solutions were tried for various subsets of the data, and there was excellent agreement among the various solutions, the spread between the computed elements being less than the standard error of those elements in almost every case. This had not been the case prior to the inclusion of the

TABLE 2

ORBITAL ELEMENTS

Element (1)	DDO (2)	All Blue Plates (3)	DDO + SP (4)
P (days)	5.5998 ± 0.0002	5.6000 ± 0.0001	5.599824 ± 0.000037
T (JD 2,440,000+)	1556.46 ± 0.16	1556.46 ± 0.16	1556.46 ± 0.16
V_0 (DDO) (km s^{-1})	−1.7 ± 0.6	−1.8 ± 0.5	−1.7 ± 0.5
V_0 (MWP + Lick)	...	+0.1 ± 0.7	...
V_0 (DAO)	...	−6.1 ± 1.3	...
V_0 (RGO)	...	+0.1 ± 1.2	...
K (km s^{-1})	72.2 ± 0.8	72.7 ± 0.6	72.2 ± 0.8
e	0.06 ± 0.01	0.049 ± 0.007	0.06 ± 0.01
ω	330° ± 10°	327° ± 9°	330° ± 10°
$a_1 \sin i$ (10^6 km)	5.549 ± 0.063	5.593 ± 0.042	5.549 ± 0.061
$f(\mathfrak{M})$ ($\mathfrak{M}_\odot$)	0.217 ± 0.007	0.222 ± 0.005	0.217 ± 0.007
ϵ (km s^{-1})	±4.39	±5.43	±4.38
Superior conjunction (JD 2,440,000+)	...	...	1561.22
Inferior conjunction (JD 2,440,000+)	...	...	1558.24

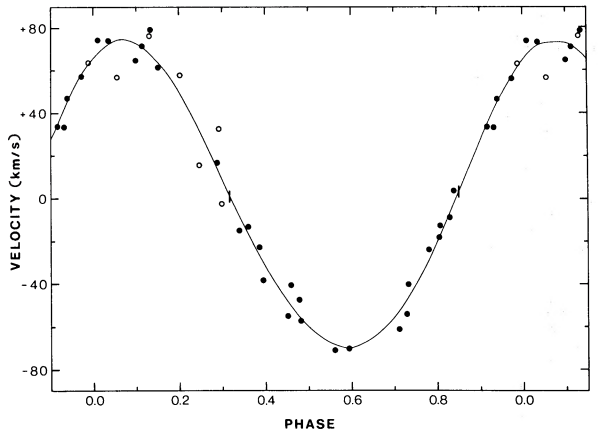

FIG. 1.—Absorption line velocity curve for HDE 226868. Only the DDO data are plotted. Open circles are points given low weight in the orbital solution because of weak or slightly out-of-focus exposures. Vertical tick marks on the velocity curve indicate phases of inferior and superior conjunction of the secondary.

new DDO and Royal Greenwich Observatory (RGO) velocities. Thus the spectroscopic orbital elements now appear to be very well determined.

The orbital elements and their standard errors from solutions using DDO velocities only and using all the blue velocities are given in columns (2) and (3) of Table 2. The quantity ϵ is the root mean square deviation of the observed velocities from the computed velocity curve. It is larger when all velocities are included because the non–DDO velocities were measured from (often much) lower dispersion spectrograms. The velocity curve computed from DDO velocities is shown in Figure 1.

c) *Period*

The apparent accuracy of the period for the first two solutions in Table 2 may be misleading since it is based on the simultaneous adjustment of all of the orbital elements and not on a long time base-line. If the period is determined separately, its uncertainty is about 10 times greater than that quoted in Table 2. The only observations from an earlier epoch (Table 3) were made by Seyfert and Popper (1941). They are so old that ambiguities of ± 1 cycle may exist in fitting them to recent observations, but they do permit some limits to be put on the period provided that the period of the system is not variable.

The Seyfert and Popper (SP) and DDO velocities have been combined and searched for significant periods in the range $5^d.590$–$5^d.610$ using an interval of

TABLE 3

EARLY EPOCH RADIAL VELOCITIES

Date	Julian Date	Phase	Velocity
1939 Sept. 26.09.....	2429532.59	0.813	−16
1940 June 15.35.....	2429795.85	0.825	− 8

TABLE 4

POSSIBLE PERIODS

P (days)	L (km s^{-1})	L' (km s^{-1})	ϵ (km s^{-1})
5.5998.....	410.4	403.4	4.39
5.5986.....	480.4	467.2	5.05
5.5972.....	535.4	524.8	6.93
5.6013.....	545.0	530.4	5.40
5.5959.....	568.0	566.6	...
5.6024.....	580.6	564.6	...
5.5978.....	611.0	466.0	...

$0^d.0001$. The search program arranged the velocities in order of phase for each test period and computed the broken string length connecting the velocities. Possible periods are those with the shorter string length. The six periods with the shortest string lengths within the period range searched are shown in Table 4 along with the broken string lengths, L and L', calculated for the DDO plus SP data and the DDO data only. The $5^d.5998$ period is clearly the best choice by this criterion. This conclusion was checked by running orbit solutions using only the DDO data and fixing the period at each of the best four periods in Table 4. The rms deviations of the velocities, ϵ, for each of these solutions are listed in Table 4 and confirm that $5^d.5998$ is the best period. A final set of orbital elements was computed using the SP and DDO velocities with the period corrected as one of the elements. These elements are given in the last column of Table 2 along with the epochs of superior and inferior conjunction of the secondary. The phases of the SP data calculated from this solution are shown in Table 4. Note that I have explicitly ignored the possibility of a variable period in this analysis.

d) *Upper Limit on i*

The mass function can be used to draw lines of constant inclination i in the $(\mathfrak{M}_2, \mathfrak{M}_1)$-plane. These are shown in Figure 2 for the domain $10\,\mathfrak{M}_\odot \leq \mathfrak{M}_1 \leq 35\,\mathfrak{M}_\odot$, the limits being taken from van den Heuvel and Ostriker (1973) and Stothers (1972), respectively. The absence of X-ray eclipses (Tananbaum *et al.* 1972; Mason *et al.* 1974) places an upper limit on the inclination. If the primary fills its Roche lobe, its radius can be approximated by

$$r = A[0.38 + 0.2 \log (\mathfrak{M}_1/\mathfrak{M}_2)]$$

for $0.2 < \mathfrak{M}_1/\mathfrak{M}_2 < 10.0$ (Paczynski 1966), where A is the semimajor axis of the relative orbit. If we define the inclination limit to be the point at which the center of the secondary begins to pass behind the primary, then $\cos i > r/A$. The mass function can be used to place this line in the $(\mathfrak{M}_2, \mathfrak{M}_1)$-plane. For HDE 226868 this limit line is almost identical to the $i = 60°$ line in the $(\mathfrak{M}_2, \mathfrak{M}_1)$-plane. The position of the eclipse limit line in the $(\mathfrak{M}_2, \mathfrak{M}_1)$-plane is insensitive to small changes in the radius of the primary.

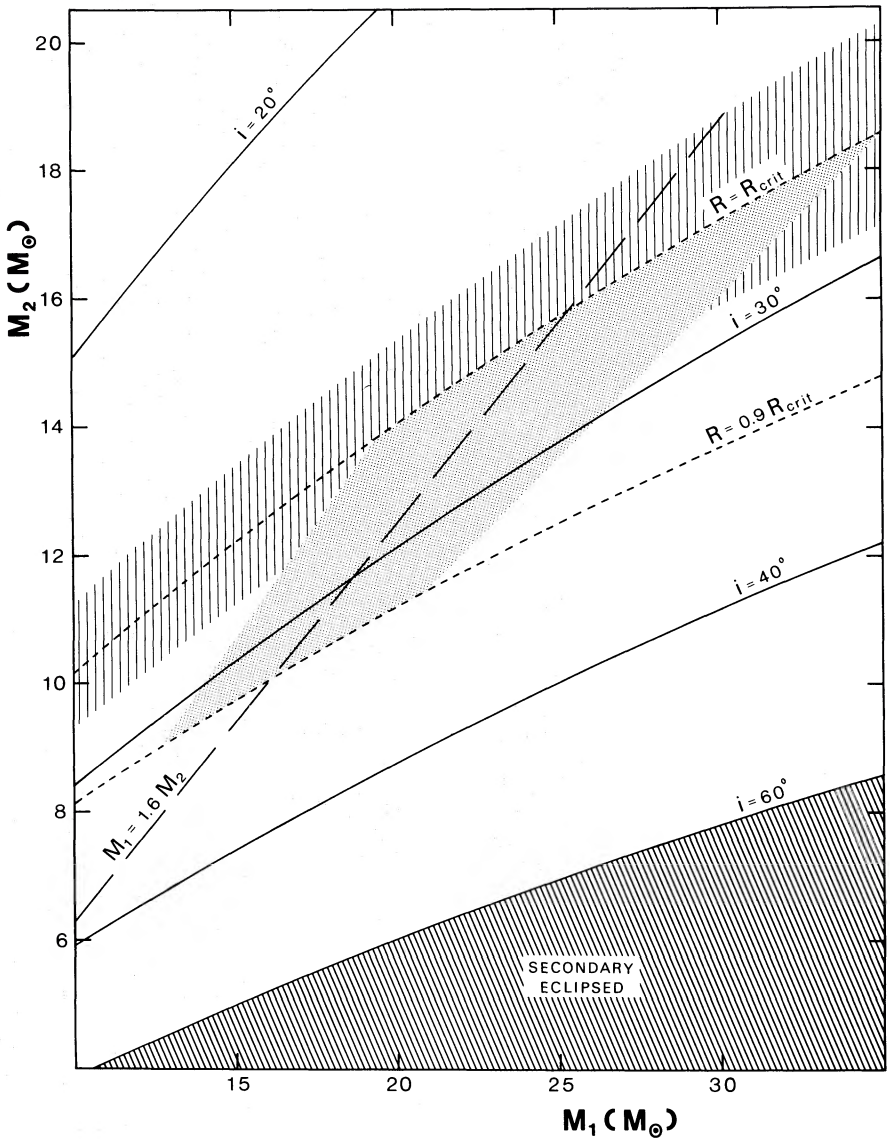

FIG. 2.—The ($\mathfrak{M}_2$, $\mathfrak{M}_1$)-plane for HDE 226868. Solid lines are lines of constant orbital inclination. Short-dashed lines are lines of constant fractional radius for the primary. The vertical shading indicates the observational uncertainty in the positioning of the $R = R_{CRIT}$ line. The stippled area is the most probable location of the HDE 226868 system.

III. THE LIGHT CURVE

HDE 226868 is an ellipsoidal variable with a B amplitude of about 0.07 mag (Cherepashchuk *et al.* 1972; Walker 1972; Lester, Nolt, and Radostitz 1973). Variations in the light curve have been reported (cf. Hutchings 1974*b*), but these appear to be small second-order effects. Hutchings (1974*b*) has used a light curve synthesis program to analyze the light curve. He derives values of e and ω close to those I have obtained from the spectroscopic data. He finds that if the primary fills its Roche lobe, then $i = 27°$–$28°$, and that there is no evidence of distortion of the light curve due to heating of the primary (secondary) by the secondary (primary). He argues that the absence of a reflection effect from the secondary indicates that it is not "normal." However, Hutchings has adopted a secondary radius of $R_2 \approx 0.2$ separation which for $i = 30°$ and $\mathfrak{M}_1/\mathfrak{M}_2 = 1.6$ corresponds to $R_2 = 8\ R_\odot$. $R_2 = 4 - 5\ R_\odot$ would be more realistic for a main-sequence star of $\sim 15\ \mathfrak{M}_\odot$.

I have repeated Hutchings's analysis using a light-curve synthesis program written by Wilson and Devinney (1971, hereinafter called WD). These calculations confirm Hutchings's results for i and the reflection effect for $R_2 = 0.2$ separation. However, for $R_2 = 0.1$ separation I find that the reflection effect is unobservable ($\Delta B < 0.01$ mag) for $i = 30°$. I also find

that the reflection effect increases with increasing inclination (R_2 fixed at 4 $R_\odot$) in such a way that $i > 45°$ is probably ruled out if the secondary is normal. Secondary surface temperatures less than $\sim$15,000 K are ruled out in the same way. Similar results have been obtained by Murdin (1974). The reflection effect results are not very dependent on the assumed primary radius unless the primary is substantially smaller (approximately a factor of 2) than its Roche lobe, but the inclination is increased when the relative primary radius is decreased.

It is possible to use the combined light and velocity curve data to solve for the secondary mass as a function of $\mathfrak{M}_1$, i, and $R_1/R_{\rm Roche}$. The light-curve synthesis program proved somewhat cumbersome in this application so a simplified method of analysis was developed. This method was checked against the more detailed light-curve synthesis program to insure that the two methods yielded the same answers.

The primary is assumed to be a rotating, limb- and gravity-darkened ellipsoid (Russell and Merrill 1952). The ellipsoidal light curve is represented by

$$l = l_{\rm max}(1 - \tfrac{1}{2}Nz\cos^2\theta),$$

where θ is the phase angle; z is the geometrical ellipticity, which depends on the mass ratio, relative radius of the star, and inclination of the orbit; and

$$N = \frac{(15 + x)(1 + y)}{15 - 5x},$$

where x and y are the limb and gravity darkening coefficients. For this analysis I shall ignore the small orbital eccentricity. The product Nz is determined from the observed light curve. Cherepashchuk *et al.* (1972) find $Nz = 0.11 \pm 0.01$. The gravity darkening coefficient, $y = 0.411$, was computed for a 30,000 K blackbody, and the limb darkening coefficient, $x = 0.4$, was chosen by fitting the linear limb darkening low to a non–LTE model atmosphere for $T_e = 27{,}000$ K, $\log g = 3.0$ (Stoeckly and Mihalas 1973). Neither coefficient is very sensitive to T or $\log g$. With these quantities specified, the inclination angle for any mass ratio is easily found from the relations

$$N(1 - b^2/a^2)\sin^2 j = Nz,$$

$$\tan i = \frac{b}{c}\tan j,$$

provided that the axes a, b, and c of the triaxial ellipsoid are known. These can be calculated from the Roche coordinates for each mass ratio. Here a is taken to be one-half the diameter of the Roche lobe (or appropriate fraction thereof) along the axis joining the two stars, and c is the semiaxis perpendicular to the orbit plane.

Once the inclination is known for a mass ratio, the mass function can be used to place the point in the $(\mathfrak{M}_2, \mathfrak{M}_1)$-plane. The short-dashed lines in Figure 2 show the relationship between $\mathfrak{M}_2$ and $\mathfrak{M}_1$ if the primary fills its Roche lobe and if nine-tenths of the Roche lobe is filled. These two lines correspond approximately to $i = 27°$ and $i = 32°$, respectively. The vertical hatching across the $R = R_{\rm CRIT}$ line indicates the uncertainty in this line due to the observational uncertainties in the mass function and Nz.

In the next section I argue that the behavior of the optical emission lines and low-energy X-ray absorption events suggests that mass loss from the primary takes place preferentially at periastron. This implies that the primary fills or nearly fills its Roche lobe, and this places an approximate lower limit of $R = 0.9\ R_{\rm CRIT}$ on the primary radius. Detailed analyses of the optical emission lines (Hutchings *et al.* 1973, 1974) indicate that the mass ratio, $\mathfrak{M}_1/\mathfrak{M}_2$, is almost certainly less than 2, and that a mass ratio of about 1.6 will satisfy all of the observations. For $1.4 \leq \mathfrak{M}_1/\mathfrak{M}_2 \leq 1.8$ the component masses fall within the stippled region in Figure 2. Indeed Figure 2 shows that for any reasonable primary mass and radius, $1 \leq \mathfrak{M}_1/\mathfrak{M}_2 \leq 2$. Bisiacchi *et al.* (1974) have also analyzed the λ4686 emission and suggested that the mass ratio is about 2.3. If $i = 30°$, this implies a primary mass greater than or equal to the upper limit for the primary's spectral type. The mass ratio range suggested here falls within the possible range allowed by the results of Bisiacchi *et al.* and leads to a primary mass estimate that is close to that for other O9.7 Iab supergiants (Stothers 1972).

Kondo (1974) has raised a number of objections to the use of the critical Roche surface in the derivation of masses. He points out that the existence and shape of the classical Roche surface depends on four assumptions: (1) circular orbit, (2) point mass components, (3) no perturbing forces, and (4) synchronous rotation. While the first assumption is violated for HDE 226868, the eccentricity is so small that I believe there will be little practical effect on the light curve calculation. Since the Roche surface has been used with some success for normal stars which are not point masses, I believe that it can be used for X-ray binaries where one component is probably effectively a point mass. The rotation velocity for HDE 226868 is $v \sin i = 140 \pm 11$ km s^{-1}. About 50 km s^{-1} of this is probably due to macroturbulence (Rosendhal 1970). If the true rotation velocity is 90 km s^{-1}, then the primary is in synchronous rotation for all models for which $\mathfrak{M}_1/\mathfrak{M}_2 \approx 1.6$. In any event the rotation will be so close to synchronism that any deviation will be unimportant (Limber 1963).

The existence of perturbing forces can seriously affect the analysis. The most likely perturbing force is radiation pressure, which would decrease the effective surface gravity of the primary. I have repeated my analysis using Schuermann's (1972) equations for the Roche surface with the effects of radiation pressure included. The decrease in the effective surface gravity depends on T_e^4, and T_e is not known with sufficient precision for HDE 226868, so various values were tried. These calculations show that radiation pressure effects are small unless the effective gravity is reduced by a factor of 10 or more. This is because the radiation pressure changes the size of the Roche surface more than the shape. For example, if the radiation pressure lowers the effective gravity to 40 percent of its original

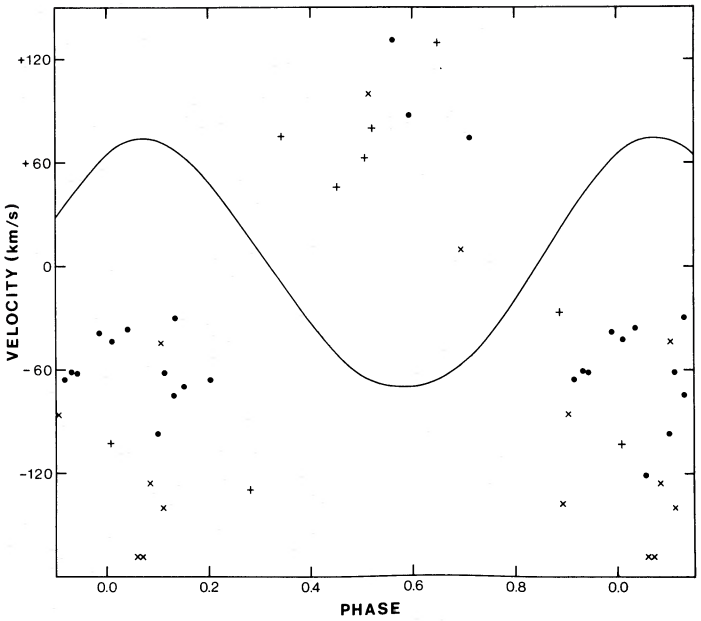

FIG. 3.—The He II λ4686 emission line velocity "curve." The calculated absorption line orbit is shown for reference. *Dots*, DDO measures; the ×'s and +'s are from Brucato and Kristian (1973) and Hutchings *et al.* (1973).

value, the derived $\mathfrak{M}_2$ values for Cyg X-1 are lowered only 10 percent. Since the gravity, $\log g \approx 3.2$, derived from the primary mass and radius values that are obtained from the light curve analysis done without the inclusion of radiation pressure is nearly identical to that derived from atmospheric analyses of OB supergiants, it is likely that we can neglect its effects in analyzing the optical data. Radiation pressure effects may *not* be negligible in the mass transfer problem.

IV. THE MASS TRANSFER

The eccentric orbit of HDE 226868 suggests that the mass loss from the primary that is indicated by the optical emission lines (Bolton 1972*b*; Hutchings *et al.* 1973, 1974) may take place preferentially near periastron and that the mass accretion rate of the secondary will therefore be highest sometime after periastron. Bolton (1972*b*) suggested this as one possible explanation for the variation of the Hβ emission strength, but the work of Hutchings *et al.* (1974) on Hα indicates that the hydrogen emission strength may vary for more complex reasons. However, several other observations point toward preferential mass loss at periastron and accretion by the secondary sometime later.

Hutchings *et al.* (1973) find that the equivalent width of the He II λ4686 emission line, which originates from a region near the secondary, peaks near apastron. Figure 3 shows that many more λ4686 velocities have been measured in the half of the orbit from periastron to apastron than in the other half. Since no such asymmetry exists in the absorption line velocities (compare Fig. 1), this implies that the line is stronger after periastron. Figure 3 also shows that there is very large scatter in the λ4686 velocities at a given orbital phase. Some of this scatter is due to the difficulty in measuring a very weak feature, but most of the scatter is probably real and due to the variable velocity and location of the emitting region in the system. Hutchings *et al.* have shown that the λ4686 emission arises from a region close to the secondary but trailing it in its orbit. This positioning is hard to understand in terms of a model in which mass is transferred in the system by a stellar wind.

Five low-energy X-ray absorption events have been found in the *Copernicus* observations of Cyg X-1 (Mason *et al.* 1974), and a sixth was detected by OSO-7 (Li and Clark 1974). Mason *et al.* note that these events occur systematically before superior conjunction. This is confirmed by DDO radial velocities obtained on JD 2,441,930.580 and 2,441,930.695 after an absorption event centered on JD 2,441,930.54. These indicate that superior conjunction was not passed until after the second plate was taken—almost 4 hours after the absorption event. Mason *et al.* have noted that the phasing of these absorption events indicates that they cannot be caused by geometric or atmospheric eclipses by the primary or by absorption by prominences. The phasing, durations, and light curves of the absorption events are also inconsistent with absorption by a stellar wind (cf. Buff and McCray 1974).

The phases of the absorption events indicate that the absorbing region trails the secondary in approximately the same way the He II λ4686 emission does, thereby suggesting a relationship between the two phenomena. Note that the low inclination derived above for the orbit requires that the absorbing region be 30°–60° out of the orbital plane. This means either that the absorbing region is very close to the secondary or (more unlikely) that it is far out of the orbital plane. The following is a possible qualitative model for the

mass transfer that can account for the above observations.

Suppose that the primary radius is such that it fills its Roche lobe near periastron. In that case there would be a brief period of mass loss ("gas streaming") through the inner Lagrangian point at periastron. This mass loss would produce a density concentration moving along the "gas stream." The properties of the density concentration (size, density, velocity, path followed in the system) will depend on the circumstances of the mass ejection (duration and amount of mass loss, velocity of ejection) which are likely to vary from cycle to cycle. Conservation of angular momentum will cause the density concentration to interact with the secondary's accretion disk at a point trailing behind the secondary in its orbit. The λ4686 He II emission would be expected to arise from the shock wave formed where the "stream" strikes the disk. Note that since the "stream" is produced by a transient overflow of the Roche lobe at periastron, the blob of ejected material is probably thicker perpendicular to the orbit plane than the typical gas stream. This thickness might be enough to account for the low-energy X-ray absorption events. Moreover, if the vertical thickness of the "stream" is comparable to or larger than the density scale height at the disk edge, the shock formed where the stream intersects the disk may tend to raise some of the "stream" gas even farther out of the orbit plane.

Periodic ejection of material at L_1 at periastron and interaction with the accretion disk $\frac{1}{2}P_{\rm orb}$ later will account for the equivalent width variations seen in the λ4686 He II emission (Hutchings *et al.* 1974 and this paper). Variability of the ejection circumstances can account for the widely fluctuating He II λ4686 velocities at the same orbital phase as well as the lack of repeatability of the Hα observations noted by Brucato and Zappala (1974). Furthermore, if the velocity of the density concentration is correct, it will interact with the accretion disk near time of superior conjunction, and an absorption event may be observed. Slightly different velocities will cause the concentration to arrive "early" or "late," when the system geometry is such that no absorption event could be observed.

The periodic ejection model is not the only possible model. Examples of other models include (i) a precessing accretion disk inclined to the orbit plane (Bardeen and Petterson 1975), and (ii) an accretion disk around a tertiary neutron star. Difficulties with this latter model are discussed below. The occasional complete absence of X-ray absorption events and their occurrence once per orbital period and not twice are hard to understand in terms of the inclined disk model. In fact, neither of the above models appears to be able to account fully for the behavior of the low-energy X-ray absorption events and the strength, velocity, and line profile behavior of the λ4686 He II and Hα emission lines. The periodic ejection model can account for all of these without invoking any phenomenon that either has not been seen in more normal binary stars (Batten 1973) or arisen as a consequence of theoretical calculations of mass transfer in binary systems (cf. Prendergast and Taam 1974).

The chief difficulty with the periodic ejection model is that calculations of stellar evolution models for massive stars filling their Roche lobes (cf. Hensberge and van den Heuvel 1974) indicate that the expected rates of mass loss are so high that the X-ray source would be quenched. Therefore, it has been argued that the mass transfer must be by a stellar wind (Morton 1967). However, if the Roche lobe overflows for only a brief time near periastron, the average rate of mass loss may be low enough to avoid the quenching problem. The success of the periodic ejection model in explaining the observations and the difficulty that the stellar wind model has in explaining the X-ray absorption events and the off-axis λ4686 emission argue strongly in favor of the periodic ejection model. The periodic ejection model does not exclude the existence of a stellar wind from HDE 226868. Observations of δ Ori (Morton 1967), which has a similar spectral type, show that it has a wind flowing outward with a velocity of 1400 km s^{-1}.

The periodic ejection model predicts that the λ4686 He II emission line should be stronger near superior conjunction when low-energy absorption events are seen than when they are not seen. There might also be some correlations between the absorption events and the velocity and line profile of the λ4686 line.

V. MODELS

a) Low-Mass Models

Two low-mass models have been proposed. Both depend on the idea that an evolved star in a binary system can be very overluminous for its mass if mass transfer has taken place. Trimble, Rose, and Weber (1973) have suggested that the system mass may be very low—on the order of 1 $\mathfrak{M}_\odot$. In their model the system also has a low luminosity and must therefore be within a few hundred parsecs of the Sun. The distance estimates of Bolton (1972*b*), which have been confirmed by Bregman *et al.* (1973) and Margon, Bowyer, and Stone (1973), exclude this possibility. In addition, the observed light curve cannot be reproduced with this model (Hutchings 1974*a*).

Van den Heuvel and Ostriker (1973) have accepted the distance estimates of the system, but they point out that the uncertainties in the distance, surface gravity, and effective temperature of HDE 226868 are such that the mass could be uncertain by factors of 2 or 3. This places a lower limit on the primary mass of about 10 $\mathfrak{M}_\odot$. The absence of X-ray eclipses then places a lower limit of 4 $\mathfrak{M}_\odot$ on the secondary mass. This might be uncomfortably low for proponents of models which include a black hole secondary, but the requirement that the primary have a radius near the critical radius in order to explain the gas streaming discussed above raises the lower limit on $\mathfrak{M}_2$ to about 8 $\mathfrak{M}_\odot$. The mass ratios derived from detailed studies of the emission lines raise the lower limits on both $\mathfrak{M}_2$ and $\mathfrak{M}_1$ still more. Thus low-mass collapsed secondaries such as neutron stars and ordinary white dwarfs are excluded. Even if the periodic ejection model is not accepted, the lower limit on the secondary mass set by the mass ratio

observations ($\mathfrak{M}_2 \approx 5.5\,\mathfrak{M}_\odot$) is comfortably above the upper limits on neutron star masses.

b) *High-Mass Models*

Two high-mass models have been suggested that involve normal main-sequence B-type secondaries. Bahcall, Rosenbluth, and Kulsrud (1973) have suggested that the system might consist of two normal stars linked by a magnetic field. If one or both of the stars were in nonsynchronous rotation, the magnetic field lines would become twisted and large amounts of magnetic energy would be stored. X-rays would be produced by the release of this energy through the breaking and reconnecting of the twisted field lines. It is impossible to say anything about the rotation velocity of the secondary star in the HDE 226868 system, but I have already noted that the primary *may* be rotating synchronously.

Fabian, Pringle, and Whelan (1974) and Bahcall *et al.* (1974) have suggested that the system might be triple rather than double. In their models a neutron star tertiary orbits B-type secondary. These models are therefore able to explain the large secondary mass and the X-ray production without using a black hole. The duplicity of the "secondary" will have no detectable effect on the primary star's velocity curve. It was noted above that an upper main-sequence B star could be included in the system without producing a detectable effect in the spectrum or the light curve. However, the triple-star model also has difficulty explaining the phasing of the low-energy X-ray absorption events. Furthermore, if the tertiary neutron star is the accreting body, the accretion disk should be gravitationally bound to it and large systematic deviations should be apparent in the λ4686 He II velocity curve. These deviations will appear as scatter about the velocity curve when it is plotted with the $5^d.6$ period. The expected scatter for a "typical" secondary-tertiary system ($P \approx 9$ hours, $\mathfrak{M}_2 + \mathfrak{M}_3 = 10\,\mathfrak{M}_\odot$) is greater than ± 120 km s^{-1} for $i \geq 30°$ and coplanar orbits. This is more than twice the scatter that has been observed (cf. Fig. 3). The difference between the observed and predicted scatter can be reduced by increasing the tertiary period and/or allowing its orbit to be noncoplanar with that of the primary. Both changes will tend to make the tertiary orbit more unstable, however. It is pointless at present to search the λ4686 He II velocities for multiple periodicities because of the small quantity of poor inhomogeneous data and the fact that most of the measures are an average of the emission line blended with the primary's absorption line (Hutchings *et al.* 1973).

Brecher and Morrison (1973) and Lamb and Van Horn (1973) have suggested that the secondary might be a differentially rotating degenerate dwarf (DRDD). These have sufficiently large gravitational fields to produce X-rays by accretion and can have masses as large as those found here for the secondary. A DRDD had a large radius compared with a black hole of the same mass. The very short time-scale variations in X-ray intensity observed from Cyg X-1 (Rothschild *et al.* 1974) could not be produced by a DRDD unless the accreted mass is channeled to a small fraction of the surface area. This might be done by a sufficiently strong magnetic field, but any magnetic field in a DRDD will be very tangled due to the rapid differential rotation and is not likely to attain the necessary strength and order to accomplish the channeling.

From the above discussion it appears that low-mass models and the DRDD model are ruled out by the observations. The triple-star model also seems to have considerable difficulty explaining all of the observations. At present there are no observational constraints on the magnetic field reconnection model, but its predictions are so vague that they almost defy observational test. The only models that are left are those in which the secondary is a black hole. None of the available observations present any difficulties for these models. In view of the numerous difficulties with the other available models, the evidence for a black hole secondary seems very strong.

I would like to thank Drs. A. P. Cowley and K. O. Mason for providing data prior to publication and Dr. R. E. Wilson for providing me with a copy of his light-curve synthesis program. I have had several conversations with Drs. J. B. Hutchings and A. P. Cowley and correspondence with K. O. Mason which have contributed greatly to the formation of the ideas presented here. The referee's comments on the original version have also been a great help in clarifying my thinking. This work was supported by a grant through the National Research Council of Canada.

REFERENCES

Bahcall, J. N., Rosenbluth, M. N., and Kulsrud, R. M. 1973, *Nature Phys. Sci.*, **243**, 27.
Bahcall, J. N., Dyson, F. J., Katz, J. I., and Paczynski, B. 1974, *Ap. J. (Letters)*, **189**, L17.
Bardeen, J. M., and Petterson, J. A. 1975, *Ap. J. (Letters)*, **195**, L65.
Batten, Alan H. 1973, *Binary and Multiple Systems of Stars* (1st ed.; Oxford: Pergamon Press), p. 166.
Bertiau, F. C., and Grobben, J. 1969, *Ric. Astr. Vaticana*, **8**, 1.
Bisiacchi, G. F., Dultzin, D., Firmani, C., and Hacyan, S. 1974, *Ap. J. (Letters)*, **190**, L59.
Bolton, C. T. 1971, *Bull. AAS*, **3**, 458.
———. 1972*a*, *Nature*, **235**, 271.
———. 1972*b*, *Nature Phys. Sci.*, **240**, 124.
Brecher, K., and Morrison, P. 1973, *Ap. J. (Letters)*, **180**, L107.
Bregman, J., Butler, D., Kemper, E., Koski, A., Kraft, R. P., and Stone, R. P. S. 1973, *Ap. J. (Letters)*, **185**, L117.
Brucato, R. J., and Kristian, J. 1973, *Ap. J. (Letters)*, **179**, L129.
Brucato, R. J., and Zappala, R. R. 1974, *Ap. J. (Letters)*, **189**, L71.
Buff, J., and McCray, R. 1974, *Ap. J. (Letters)*, **188**, L37.
Cherepashchuk, A. M., Lyutyj, V. M., and Sunyaev, R. A. 1973, *Astr. Zh.*, **50**, 3.
Cowley, A. P. 1974, private communication.
Fabian, A. C., Pringle, J. E., and Whelan, J. A. J. 1974, *Nature*, **247**, 351.
Hensberge, G., and van den Heuvel, E. P. J. 1974, *Astr. and Ap.*, **33**, 311.
Hutchings, J. B. 1974*a*, *Ap. J.*, **188**, 341.
———. 1974*b*, *Ap. J. (Letters)*, **193**, L61.

Hutchings, J. B., Crampton, D., Glaspey, J., and Walker, G. A. H. 1973, *Ap. J.*, **182**, 549.
Hutchings, J. B., Cowley, A. P., Crampton, D., Fahlmann, G., Glaspey, J. W., and Walker, G. A. H. 1974, *Ap. J.*, **191**, 743.
Kippenhahn, R. 1969, *Astr. and Ap.*, **3**, 83.
Kondo, Y. 1974, *Ap. and Space Sci.*, **27**, 293.
Lamb, D. Q., and Van Horn, H. M. 1973, *Ap. J.*, **183**, 959.
Lester, D. F., Nolt, I. G., and Radostitz, J. V. 1973, *Nature Phys. Sci.*, **241**, 125.
Li, F. K., and Clark, G. W. 1974, *Ap. J.* (*Letters*), **191**, L27.
Limber, D. N. 1963, *Ap. J.*, **138**, 1112.
Margon, B., Bowyer, S., and Stone, R. P. S. 1973, *Ap. J.* (*Letters*), **185**, L113.
Mason, K. O., Hawkins, F. J., Sanford, P. W., Murdin, P., and Savage, A. 1974, *Ap. J.* (*Letters*), **192**, L65.
Morton, D. C. 1967, *Ap. J.*, **147**, 1017.
Murdin, P. 1974, preprint.
Paczynski, B. 1966, *Acta Astr.*, **16**, 1.
Prendergast, K. H., and Taam, R. E. 1974, *Ap. J.*, **189**, 125.
Rosendhal, J. D. 1970, *Ap. J.*, **159**, 107.
Rothschild, R. E., Boldt, E. A., Holt, S. S., and Serlemitsos, P. J. 1974, *Ap. J.* (*Letters*), **189**, L13.
Russell, H. N., and Merrill, J. E. 1952, *Contr. Princeton Univ. Obs.*, **26**, 1.
Schuermann, D. W. 1972, *Ap. and Space Sci.*, **19**, 351.
Seyfert, C., and Popper, D. M. 1941, *Ap. J.*, **93**, 461.
Smith, H. E., Margon, B., and Conti, P. S. 1973, *Ap. J.* (*Letters*), **179**, L125.
Stoeckly, T. R., and Mihalas, D. 1973, *NCAR Tech. Note*, No. STR84.
Stothers, R. 1972, *Ap. J.*, **175**, 431.
Tananbaum, H., Gursky, H., Kellogg, E., Giacconi, R., and Jones, C. 1972, *Ap. J.* (*Letters*), **177**, L5.
Trimble, V., Rose, W. K., and Weber, J. 1973, *M.N.R.A.S.*, **162**, 1P.
van den Heuvel, E. P. J., and Ostriker, J. P. 1973, *Nature Phys. Sci.*, **245**, 99.
Walborn, N. R. 1973, *Ap. J.* (*Letters*), **179**, L123.
Walker, E. N. 1972, *M.N.R.A.S.*, **160**, 9P.
Webster, B. L., and Murdin, P. 1972, *Nature*, **235**, 37.
Wilson, R. E., and Devinney, E. J. 1971, *Ap. J.*, **166**, 605 (WD).

C. T. BOLTON: David Dunlap Observatory, University of Toronto, Richmond Hill, Ontario, Canada